Agricultural and Forest Meteorology 149 (2009) 1447–1459

Contents lists available at ScienceDirect

Agricultural and Forest Meteorology

journal homepage: www.elsevier.com/locate/agrformet

Controls over ozone deposition to a high elevation subalpine forest

Andrew A. Turnipseed [a,*], Sean P. Burns [b,c], David J.P. Moore [d], Jia Hu [b], Alex B. Guenther [a], Russell K. Monson [b,e]

[a] Atmospheric Chemistry Division, National Center for Atmospheric Research, 3450 Mitchell Lane, Boulder, CO 80301, USA
[b] Department of Ecology and Evolutionary Biology, Campus Box 334, University of Colorado, Boulder, CO 80309, USA
[c] Mesoscale and Microscale Meteorology, National Center for Atmospheric Research, 3450 Mitchell Lane, Boulder, CO 80305, USA
[d] Department of Geography, King's College London, Strand, London WC2R 2LS, UK
[e] Cooperative Institute for Research in Environmental Sciences, University of Colorado, Boulder, CO, 80309, USA

ARTICLE INFO

Article history:
Received 18 June 2008
Received in revised form 7 April 2009
Accepted 8 April 2009

Keywords:
Ozone deposition
Eddy covariance
Coniferous forest
Stomatal conductance

ABSTRACT

Ecosystem level ozone (O_3) fluxes during four different years were examined at a subalpine forest site in the Colorado Rocky Mountains. The local mountain–valley wind system and the proximity of the Denver Metropolitan area leads to high summertime ozone episodes on many afternoons. The timing between these episodes and the ecosystem processes controlling photosynthesis during the growing season plays a critical role in determining the amount of ozone deposition. Light and vapor pressure deficit (VPD) were the most dominant environmental drivers controlling the deposition of O_3 at this site through their influence on stomatal conductance. 81% of the daytime O_3 uptake was predicted to occur through the stomata. Stomatal uptake decreased at high VPD and temperatures leading to an overall decrease in O_3 flux; however, we did observe a non-stomatal conductance for O_3 that increased slightly with temperature before leveling off at higher values. During the growing season, O_3 deposition fluxes were enhanced after midday precipitation events and continued at elevated levels throughout the following night, implying a role for surface wetness. From nighttime data, evidence for both the presence of water films on the needles and non-closure of the plant stomata were observed. During the winter (non-growing) season, the ozone deposition velocity showed a consistent dependency on the latent heat flux. Although the mechanism is unclear, it is apparent that precipitation events play a role here through their influence on latent heat flux.

1. Introduction

Increases in ground-level ozone (O_3) have been of great concern over the past 100 years (Vingarzan, 2004 and references therein). These increases are due mainly to the photochemical production of O_3 from anthropogenically emitted nitrogen oxides (NO_x) combining with hydrocarbons (both anthropogenic and biogenic). Since O_3 is a respiratory irritant in humans (Curtis et al., 2006) and deleterious to plant growth (Jacobson, 1982; Heck et al., 1984; Pye, 1988; Chappelka and Samuelson, 1998), it is critical to fully understand both the production and loss mechanisms of tropospheric O_3 in order to accurately arrive at mitigation strategies (Jacobson, 1982; US EPA, 1996; Führer and Booker, 2003; Bytnerowicz et al., 2004).

A major loss process for O_3 is surface deposition. A large fraction of this deposition occurs through direct uptake by vegetation through the stomatal pores (Wesely, 1989; Wesely and Hicks, 2000). As quantitation of this loss is important toward predicting plant damage caused by O_3, it has been argued that O_3 concentration alone (as measured by many monitoring networks) is not adequate to predict damage to vegetation (US EPA, 1996; Musselman and Massman, 1999; Cieslik, 2004; Karlsson et al., 2004; Massman, 2004; Emberson et al., 2007). To this end, there have been numerous studies of ozone deposition to vegetation over the past 50 years (e.g., Regener, 1957; Wesely et al., 1978; Fuentes et al., 1992; Coe et al., 1995; Munger et al., 1996; Lamaud et al., 2002; Kurpius and Goldstein, 2003; Mikkelsen et al., 2004; Hogg et al., 2007), and these results have formed the basis for deposition models aimed at predicting vegetative ozone uptake (Wesely, 1989; Zhang et al., 2002).

Although a significant fraction of the O_3 flux occurs through plant stomata, other pathways (hereafter grouped together as "non-stomatal") appear to be important in many conditions (Kurpius and Goldstein, 2003; Hogg et al., 2007). Environmental factors such as temperature, humidity and light are known to have important impacts in regulating stomatal uptake; however, they also likely play a role in non-stomatal uptake as well. For example, the non-stomatal portion of O_3 uptake has been shown to be

* Corresponding author. Tel.: +1 303 497 1448; fax: +1 303 497 1400.
E-mail address: turnip@ucar.edu (A.A. Turnipseed).

0168-1923/$ – see front matter © 2009 Elsevier B.V. All rights reserved.
doi:10.1016/j.agrformet.2009.04.001

sensitive to temperature and attributed to either surface thermal decomposition (Fowler et al., 2001), reactions of O_3 on surfaces (Fruekilde et al., 1998), or reactions with reactive species emitted by the ecosystem (e.g., NO and hydrocarbon species) (Kurpius and Goldstein, 2003; Mikkelsen et al., 2004; Hogg et al., 2007). Surface wetness also appears to play a role in O_3 deposition (Altimir et al., 2006); however, this effect can be variable depending on the ecosystem studied (Massman, 2004).

The Niwot Ridge AmeriFlux site lies in a subalpine conifer forest in the Rocky Mountains to the west of the Denver Metropolitan area. It is situated on the leeward side of the mountains and experiences a mountain–valley type of wind system, resulting in upslope air flows from the Front Range urban corridor. Many studies have documented the occurrence of high concentrations of O_3 and other pollutants in areas surrounding Niwot Ridge during these 'upslope' conditions (Fehsenfeld et al., 1983; Parrish et al., 1986a,b; Ridley et al., 1990). However, there have not been any studies with the aim of quantitatively measuring the flux of O_3 into the subalpine forest ecosystem under these affected conditions. In the present work, we describe the results from 4 years of ecosystem level O_3 flux measurements made at the Niwot Ridge AmeriFlux site with the goals of understanding: (1) the timing of upslope events at higher elevations and the degree to which they occur simultaneously with periods of high plant activity (i.e., high capacity for stomatal uptake); (2) separation of the stomatal and non-stomatal contributions to the O_3 flux to the forest; and (3) the environmental controls over the stomatal and non-stomatal components of the flux.

2. Experimental

2.1. Site description

The study was conducted at the Niwot Ridge AmeriFlux site in the Roosevelt National Forest in the Rocky Mountains of Colorado located at 40°1′58.4″N and 105°32′47.0″W at an elevation of 3050 m. Thorough descriptions have been presented by Monson et al. (2002) and Turnipseed et al. (2002, 2003) and only a brief summary will be given here. Measurements were made from a 27-m scaffolding tower within a coniferous subalpine forest. Table 1 lists the dominant species and other important descriptive parameters that have been reported for this site.

Table 1
Forest characteristics[a].

Species	Lodgepole pine Engelmann Spruce Subalpine Fir	*Pinus contorta* *Picea engelmannii* *Abies lasiocarpa*
Leaf area index	LAI	4.2 m^2 m^{-2} (one-sided, seasonal maximum)
Canopy height	h_c	11.4 m
Displacement height	d	7.8 m
Gap fraction	GF	17%
Aerodynamic roughness	z_0	1.6 m
Stem density	S_d	4000 stems ha^{-1}

From Monson et al. (2002) and Turnipseed et al. (2002, 2003).

The mountain–valley winds which predominate at this site have a profound effect on atmospheric O_3 dynamics. Thermally induced upslope flows from the east occur on many summer afternoons (~1/3 of the days) bringing high concentrations of anthropogenic pollutants from the Denver/Boulder Metropolitan area (Fehsenfeld et al., 1983). The upward movement of warm, moist air from lower elevations during these upslope events also often contributes to convective thunderstorm activity. Although upslope flow can also result from synoptic storm systems which are also accompanied by precipitation, this is less common during the summer growing season (Losleben et al., 2000). Despite the clear importance of upslope winds to O_3 dynamics at the study site, the predominant wind direction is from the west, including most nocturnal flows, which are often katabatic in nature (Brazel and Brazel, 1983; Turnipseed et al., 2003). Westerly flow is not impacted by any nearby anthropogenic sources.

2.2. Methodology

Ozone fluxes were measured by the technique of eddy covariance. Three-dimensional wind velocities were measured with a sonic anemometer (Campbell Scientific, CSAT-3) located at 21.5 m and recorded at 10 Hz using a datalogger (Campbell Scientific, CR23x). Fast fluctuations in O_3 concentrations were measured at 10 Hz with a sensor similar to that described by Güsten et al. (1992) and Güsten and Heinrich (1996) (Fig. 1). Air was drawn at a constant rate of 7 L min^{-1} through a 4 m Teflon

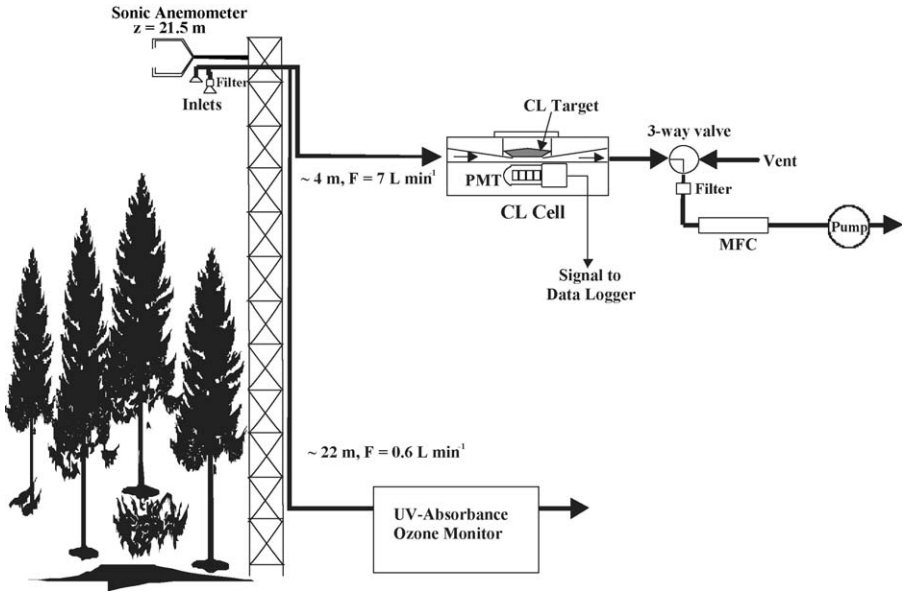

Fig. 1. Schematic of the instrumental setup and the fast O_3 sensor. MFC = mass flow controller, CL = chemiluminescence, F = flow rate, PMT = photomultiplier tube.

inlet line located at the base of the sonic anemometer head. The sampled air was then passed over a dye-impregnated (Coumarin 152) target where O_3 was detected from the chemiluminescent reaction of O_3 with the dye. Light emissions were measured with a photomultiplier tube (Hamamatsu, 1P28) and the ensuing photocurrent was converted to an analog voltage and measured using the same datalogger collecting the sonic anemometer data. Other atmospheric species have been shown not to produce light or interfere with the O_3 measurement (Güsten et al., 1992). Laboratory tests indicted that the response time ($1/e$) to a step change in O_3 concentrations was <0.2 s with a measurement precision of ~0.4 ppbv making it suitable for eddy covariance measurements.

Over time, as the dye reacts with O_3, the sensitivity of the sensor changes; therefore, a slower, more stable UV-absorption O_3 monitor (TECO Model 49C) was operated concurrently with the fast sensor for calibration purposes and as a reference monitor; the analog voltage from this sensor was also recorded by a datalogger (Campbell Scientific, CR23x). The fast O_3 sensor was zeroed every 4 h by shutting off the air flow through the target area, resulting in the rapid reaction of all the O_3 near the surface of the target (<3 s). The calibration of the fast sensor involved breaking a given 30 minute flux averaging period into six subsets (5 min each) and relating the average signal of the fast sensor (minus the zero signal) from each of these subsets to the O_3 concentration measured with the slow sensor. Typical sensitivities ranged from 2 to 6 mV/ppbv. When the sensitivity dropped below a value of 1.9 mV/ppbv (usually after 1–2 weeks of use), the target was replaced. If the sensitivity was ≥1.9 mV/ppbv and varied less than 15% over the 30 min period, data was assumed to be valid for further analysis. The calibration of the slower UV-absorption monitor was checked periodically by comparison with other UV-absorption based instruments, both in the laboratory and in the field, and found to agree within ±5%.

Mean concentration values and fluxes were calculated as a block average over a half-hour time period. Lag times between the fast O_3 signal and the vertical wind velocity, w, caused by transit time in the inlet tubing were calculated by varying the lag between the two time series and finding the maximum correlation. Signals were shifted in time by this lag (typical lag = 0.4 s) relative to w before covariances were calculated. The wind coordinate frame was rotated using the planar fit method described by Wilczak et al. (2001) which has been shown to be effective for this site (Turnipseed et al., 2003). Ozone fluxes were then calculated from the covariance between the vertical wind velocity and the O_3 density, ρ_o, measured with the fast sensor. Co-spectral analysis (data not shown) comparing $\overline{w'\rho_o'}$ to that of the kinematic vertical turbulent heat flux from the sonic anemometer ($\overline{w'T'}$) indicated that the O_3 fluctuations at frequencies >1 Hz were within the random noise of the instrument; therefore, we corrected for this high frequency loss by a factor of $\overline{w'T'}/\overline{w'T'}_f$ where $\overline{w'T'}_f$ was the covariance after the temperature time series was filtered using an exponential low pass filter with a cutoff frequency of 1.5 Hz. On average, the correction was <10% for daytime fluxes. Flux data were also omitted during periods of very low turbulence intensity (when friction velocity, $u^* < 0.2$ m s^{-1}), as well as during violations of tests for nonstationarity and integral wind statistics (Foken and Wichura, 1996). This resulted in approximately 16% of the daytime flux periods and 68% of the nighttime data (primarily for low u^*) being omitted.

Continuous meteorological (temperature, humidity, wind speed/direction, radiation, etc.) and flux (sensible and latent heat, CO_2 flux) measurements, both within and above the canopy, were provided by the Niwot Ridge AmeriFlux site as part of their ongoing studies of ecosystem carbon cycling in the Rocky Mountains. These measurements have been described in previous publications (Monson et al., 2002; Turnipseed et al., 2002) and a thorough description of the instrumentation, methodology and measurement heights is given at http://public.ornl.gov/ameriflux/Site_Info/siteInfo.cfm?KEYID=us.niwot_ridge.01.

Sap flow measurements were made in all three conifer species (a total of nine trees) using the heat ratio method and sensors described in Burgess et al. (2001). Each sensor included a heater (which emits a heat pulse) located between two thermocouples (which detect the dispersion of the heat pulse) inserted vertically within the tree bole at breast height. Multiple sensors were positioned radially within a single tree. Data collection and control over heat pulsing was accomplished using dataloggers with integrated multiplexers (Campbell Scientific, model CR10X and AM416, respectively).

2.3. Measurement periods

Growing season measurements presented here were taken from 2002 (June–August), 2003 (May–September), and 2005 (May–August). Instrumental problems curtailed our 2004 measurements to only the early season (May–June). Fluxes were measured semi-continuously as targets were not always replaced before their sensitivity degraded. The time coverage for flux measurements during the growing season was ~62%, with a minimum of 2.5 weeks of flux measurements/month. Ozone fluxes were measured in several "campaign mode" studies during the non-growing season (~November to April). In these cases, flux measurements were made at different times, to capture different aspects of the annual ecosystem cycle including springtime initiation of forest net CO_2 uptake (April–May, 2004, 2005), fall cessation of net CO_2 uptake (September–October, 2003, 2004) and winter dormancy (November, 2003, January–March, 2004, March, 2005).

2.4. Data analysis

Deposition velocities were determined as $V_d(O_3) = -F_o/\bar{\rho}_o$ where $\bar{\rho}_o$ is the mean O_3 density and F_o is the flux. For this study, we used a single-layer resistance model to relate the deposition to a series of individual component resistances which reflect physical constraints on the flux (Wesely, 1989; Wesely and Hicks, 2000).

$$\frac{1}{V_d(O_3)} = R_a(z-d) + R_b + R_c. \tag{6}$$

Here, R_a is the stability-corrected aerodynamic resistance to mass transfer at the measurement height (Garland, 1977; Turnipseed et al., 2006) of $z - d$ = 13.7 m (Table 1), and R_b is the resistance to mass transfer across the laminar sublayer near the surfaces. We have used the formulation for R_b following the equations provided by Hicks et al. (1987). The value of R_c is the total surface resistance and is obtained via difference between the reciprocal of the measured deposition velocity and the sum of R_a and R_b.

Over vegetation, O_3 can be deposited either through plant stomata or to plant or ground surfaces. By estimating the average canopy stomatal resistance (R_{st}), we can further separate R_c into a set of parallel resistances (or their inverse, conductances) (Wesely, 1989):

$$\frac{1}{R_c} = \frac{1}{R_{st}} + \frac{1}{R_{ns}} \tag{9}$$

where R_{ns} represents all non-stomatal processes. In terms of conductances:

$$\frac{1}{R_c} = G_c, \qquad \frac{1}{R_{st}} = G_{st}, \qquad \frac{1}{R_{ns}} = G_{ns}, \qquad G_c = G_{st} + G_{ns} \tag{10}$$

The non-stomatal processes include deposition to cuticular surfaces, elements in the lower canopy (e.g., branches, bark) and to the ground surface. However, this definition also encompasses

the possibility of other loss processes (e.g., chemical reactions) below the sensor height.

The separation of the stomatal and non-stomatal components of scalar uptake for dry canopies is typically estimated either relative to CO_2 uptake (Büker et al., 2007), transpiration flux (Monteith and Unsworth, 1990) or by empirical relationships (Jarvis, 1976; Büker et al., 2007). For O_3, it is typically derived relative to the water vapor flux, assumed to come primarily from plant transpiration. Gerosa et al. (2007) have recently reviewed the two most common methods used to estimate the canopy-level stomatal resistance: (1) resistance analogies used to obtain the vapor pressure deficit at the scalar (temperature and water vapor) roughness length, z'_0, which is assumed to be equivalent to that at the leaf surface (Thom, 1975; Monteith and Unsworth, 1990), denoted as the Evaporative/Resistance (ER) method:

$$R_{st}(O_3) = D_{rat}\left(\rho c_p \frac{\lfloor e_{sat}(T(z'_0)) - e(z'_0)\rfloor}{\gamma\lambda E_T} - R_T\right), \quad (11)$$

and (2) the inverted form of the Penman–Monteith equation (PM method):

$$R_{st}(O_3) = D_{rat}R_{st}(H_2O) = D_{rat}\left(\left[\frac{R_T s(R_n - G - \lambda E_T) + \rho c_p(e_{sat}(T_{z=21\,m}) - e_{z=21\,m})}{\gamma\lambda E_T}\right] - R_T\right). \quad (12)$$

Here, D_{rat} is the ratio of diffusion coefficients of H_2O to O_3 (1.65, Gerosa et al., 2003), R_T is the sum of the aerodynamic and sublayer resistances for water vapor ($R_a + R_b$), R_n is net radiation, G is the soil heat flux, s is the slope of the saturation vapor curve (de_{sat}/dT), ρ is atmospheric density, E_T is the transpiration water vapor flux, γ is the psychrometric constant, c_p is the molar heat capacity of air, and λ is the latent heat of vaporization. Eqs. (11) and (12) both rely on the measurement of the water vapor pressure deficit ($VPD \equiv e_{sat}(T) - e$, e_{sat} and e are the saturation and ambient water vapor pressures, respectively) at either the measurement height, z, or at the leaf surface, z'_0. With the assumption of a balanced surface energy budget, these two approaches are essentially identical (Monteith and Unsworth, 1990; Gerosa et al., 2007) and have been shown to give reasonable agreement in the stomatal/non-stomatal partitioning of O_3 fluxes (Gerosa et al., 2007). We have used and compared both of these methods (as well as some of the variations described in Gerosa et al., 2007) in separating the stomatal and non-stomatal contributions to the observed O_3 flux.

Both of the above formulations require the measurement of the transpiration flux, λE_T. However, what is measured above the canopy is the total water vapor flux (or latent heat flux, λE), which includes contributions from soil evaporation (λE_E). In this work, we have used two independent methods to estimate the partitioning of the latent heat flux into its soil and vegetation components. The first method is based completely on measured eddy covariance fluxes above ($z = 21.5$ m) and below ($z = 2.5$ m) the canopy: $\lambda E_T = \lambda E_{z=21.5\,m} - \lambda E_{z=2.5\,m}$ and assumes that $\lambda E_{z=2.5\,m}$ represents the water flux due to evaporation from the soils. The second method combines measured latent heat fluxes with the SIPNET ecosystem process model (Moore et al., 2008) which uses an optimization scheme to determine carbon and water flux partitioning conditioned on eddy flux observations. This analysis was based on the assimilation of 7 years of half-daily averaged fluxes of both λE and net ecosystem CO_2 exchange (NEE), and validated against measurements of λE_T made independently using sap flow techniques. As the SIPNET model is based on optimization to half-daily values, it does not always capture hour-to-hour flux variations well; therefore, we used the fractional partitioning of ($\lambda E_T/\lambda E$) derived from SIPNET, and multiplied it by the measured 30-min λE to estimate λE_T. A comparison of λE_T derived from these two methods is shown in Fig. 2 for the summer of 2003. As seen in the figure, on average the two methods predict similar behavior of λE_T. For midday summer fluxes, the average $\lambda E_{z=2.5\,m}/\lambda E_{z=21.5\,m}$ was typically about 8–10%, whereas, combining SIPNET with measured $\lambda E_{z=21.5\,m}$ predicted a slightly larger evaporative fraction ($\lambda E_E/\lambda E \sim 15$–18%). However, both of these estimates are well within the range of values found in other studies of conifer canopies (Kelliher et al., 1993; Schäfer et al., 2002). We feel that the combination of the model with measured latent heat fluxes above the canopy led to a more robust data set as the comparison of within and above-canopy fluxes of water vapor can be problematic (for example, mismatch of flux footprints, decoupling of above and within-canopy air during stable periods, understory transpiration). Therefore the results presented below are derived using the SIPNET approach.

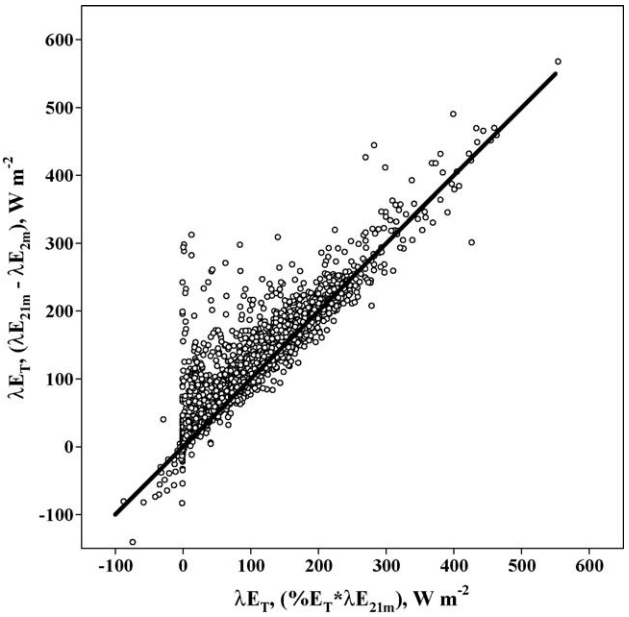

Fig. 2. Calculated transpiration fluxes (λE_T) derived from the difference in measured latent heat fluxes at 21.5 and 2.5 m compared to λE_T obtained from the SIPNET model partitioning. The line drawn is the 1:1 line.

3. Results and discussion

3.1. Summertime upslope flow and O_3 deposition

During the summer growing season, O_3 fluxes are regulated by both plant activity (stomatal uptake) and meteorology. Afternoon upslope winds bring air containing processed pollutants from the Denver metropolitan corridor, along with elevated concentrations of O_3 that tend to drive higher deposition rates. Fig. 3 shows a time series from August 2–5, 2003 which was representative of typical high pollution, upslope days. The mountain–valley wind signature was clearly evident in the wind direction data (Fig. 3b), whereby nocturnal winds from the west (downslope) transitioned during the morning to upslope flow from the east. As reduced solar heating weakened the upslope flow in the late afternoon, downslope drainage winds were re-established. Prolonged upslope flow and clear skies (as in Fig. 3) tends to facilitate O_3 production and transport to the site. Transitions to upslope flow can also occur later in the day and are typically accompanied by rapid increases in O_3 concentrations. Observed O_3 fluxes were in good agreement with previous measurements over a similar subalpine forest (Zeller and Nikolov, 2000) and tended to be

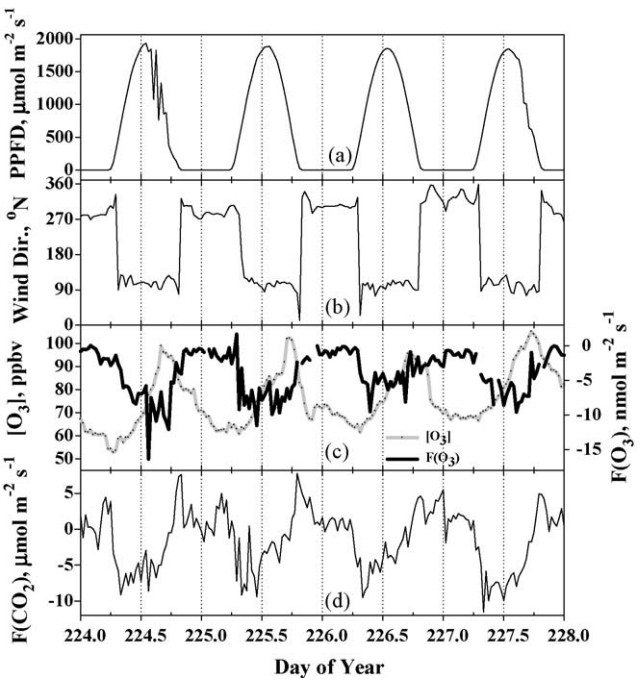

Fig. 3. Time series of (a) incoming photosynthetic photon flux density (PPFD), (b) wind direction, (c) O_3 concentration and flux and (d) CO_2 flux during a 4-day period in August, 2003 which experienced strong daytime upslopes and high O_3 photochemical production.

correlated with patterns in the net CO_2 flux [$F(CO_2)$]. The peak in $F(O_3)$, however, tended to occur later in the day than that for $F(CO_2)$, driven by increasing O_3 concentration. Late afternoon reductions in $F(O_3)$ were correlated with reductions in the photosynthetic photon flux density (PPFD) and higher VPDs (data not shown); although ozone concentration continues to rise until nearly 18:00 local time. This is likely due to reductions in stomatal conductance as evidenced by decreasing $F(CO_2)$. This effectively limits the observed ozone flux into the plant even with increasing ozone concentration. Therefore, this offset in timing tends to lessen the impact of anthropogenic ozone from the Denver Metro area on high elevation Front Range forests to some degree.

3.2. Factors influencing $V_d(O_3)$

From Fig. 3 it is obvious that light exhibits a major control over $F(O_3)$ in a similar fashion to $F(CO_2)$. However, the differences described in the last section suggest that there are differences in how these environmental drivers (PPFD, temperature, VPD) influence ozone deposition. However, these environmental factors are often not independent from each other (e.g., high PPFD and high VPD often occur along with high temperature) and, the actual controlling variables are not always easily deciphered. The Niwot Ridge site has the advantage that there are some important differences between the two primary wind regimes (upslope and downslope) and these differences can be used to deduce which environmental factor(s) exerts the most influence on observed measurements. One clear observation that was apparent during each year of our observations was that $V_d(O_3)$ was higher during upslope periods. Over the entire growing season, average daytime $V_d(O_3)$ were statistically smaller by 17% ($p < 0.01$, two-tailed t-test) during periods of downslope winds (see Table 2). Average temperatures were nearly the same during upslope and downslope flow regimes; however, mean wind speed (U) was smaller and relative humidity (RH) was higher during upslope flow (Table 2). Lower wind speeds could suggest lower measured fluxes due to

Table 2
Median daytime values of environmental drivers and fluxes during the growing season for different flow regimes (upslope and downslope).

Flow direction	Temperature (°C)	RH/VPD (%/kPa)	U (m s^{-1})	λE_T (W m^{-2})	O_3 (ppbv)	$F(O_3)$ (nmol m^{-2} s^{-1})	$V_d(O_3)$[a] (mm s^{-1})	G_c (mm s^{-1})	G_{st}[b] (mm s^{-1})	G_{ns} (mm s^{-1})	G_{st}/G_c
Upslope	13.5	49%/0.98	2.6	94.4	62.0 ± 0.4 (2452)	−7.97 ± 0.11 (2452)	4.33 ± 0.07 (2452)	4.73 ± 0.10 (2452)	3.69 ± 0.10 (2145)	0.75 ± 0.09 (2145)	0.80 ± 0.03 (2145)
Downslope	14.0	34%/1.26	4.2	115.9	55.7 ± 0.1 (3129)	−6.01 ± 0.08 (3129)	3.59 ± 0.05 (3129)	3.81 ± 0.07 (3129)	3.08 ± 0.07 (2818)	0.71 ± 0.06 (2818)	0.81 ± 0.02 (2818)
All data	13.8	41%/1.13	3.4	104.5	58.4 ± 0.2 (5883)	−6.74 ± 0.07 (5883)	3.88 ± 0.04 (5883)	4.20 ± 0.06 (5883)	3.29 ± 0.06 (5200)	0.73 ± 0.05 (5200)	0.81 ± 0.02 (5200)

[a] Errors are the standard error ($\sigma/\sqrt{N}$). The values in parentheses are the number of 30 minute flux averaging periods.
[b] Using the ER method (see text) assuming that $T_{8\,m} = T_{leaf}$.

reduced turbulent transport (Turnipseed et al., 2002), yet larger fluxes were observed. Greater deposition rates are consistent with higher relative humidity (or lower VPD) which lead to greater stomatal conductances.

Fig. 4 shows plots of how daytime $V_d(O_3)$ and transpiration latent heat fluxes (λE_T) behave as a function of the major environmental drivers (light, temperature, VPD). These trends were consistent for each year studied. λE_T tends to increase with incident PPFD (Fig. 4b). As VPD also increases steadily with PPFD (data not shown), this suggests regulation over stomatal openings. In turn, $V_d(O_3)$ shows only a small variation over most of the range (PPFD < 1700 μmol m^{-2} s^{-1}). However, $V_d(O_3)$ tends to be consistently higher during periods of upslope flow ($p < 0.01$ for PPFD > 500 μmol m^{-2} s^{-1}) contrary to λE_T. Since humidity is consistently higher for upslope flow, this suggests greater stomatal conductances during these periods. The behavior of $V_d(O_3)$ as a function of temperature is similar to that previously published for gross photosynthesis rate at this site (Huxman et al., 2003), exhibiting a maximum and then declining at higher temperatures. The majority of data lies between 9 and 16 °C (Fig. 4d). Within this range, λE_T for upslope and downslope flow regimes are statistically the same ($p > 0.10$) and, yet we observed higher $V_d(O_3)$ during the more humid upslope flows ($p < 0.01$). At higher temperatures, there is little wind direction difference in $V_d(O_3)$; however, λE_T is smaller during upslope periods. These observations are, again, all consistent with greater average stomatal conductances during upslope flow.

As seen in Fig. 4e, $V_d(O_3)$ shows a steady decrease with VPD, consistent with lower stomatal conductances during drier conditions. Measurements during both upslope and downslope flows collapse onto a single line, showing no statistical differences in each of the bins ($p > 0.10$). At high VPD, there are wind direction divergences in the predicted λE_T that are not reflected in $V_d(O_3)$. However, one must keep in mind the non-stomatal component of the ozone flux which we examine in the next section.

3.3. Stomatal and non-stomatal contributions to O_3 deposition

From the relationships shown in Figs. 3 and 4, we can infer a strong role for stomatal conductance as a factor controlling O_3 uptake. In this study, we estimated the stomatal resistance during daylight hours (07:00–19:00) relative to the water vapor flux, as we have more direct methods for ascertaining the reliability of these flux measurements (e.g., multiple instrumentation systems and surface energy budgets, Turnipseed et al., 2002). Using the ER method (Section 2.4) and assuming that ambient air temperature measured within the canopy ($z = 8$ m) was equivalent to leaf temperature, Fig. 5 shows a plot of modeled stomatal conductance

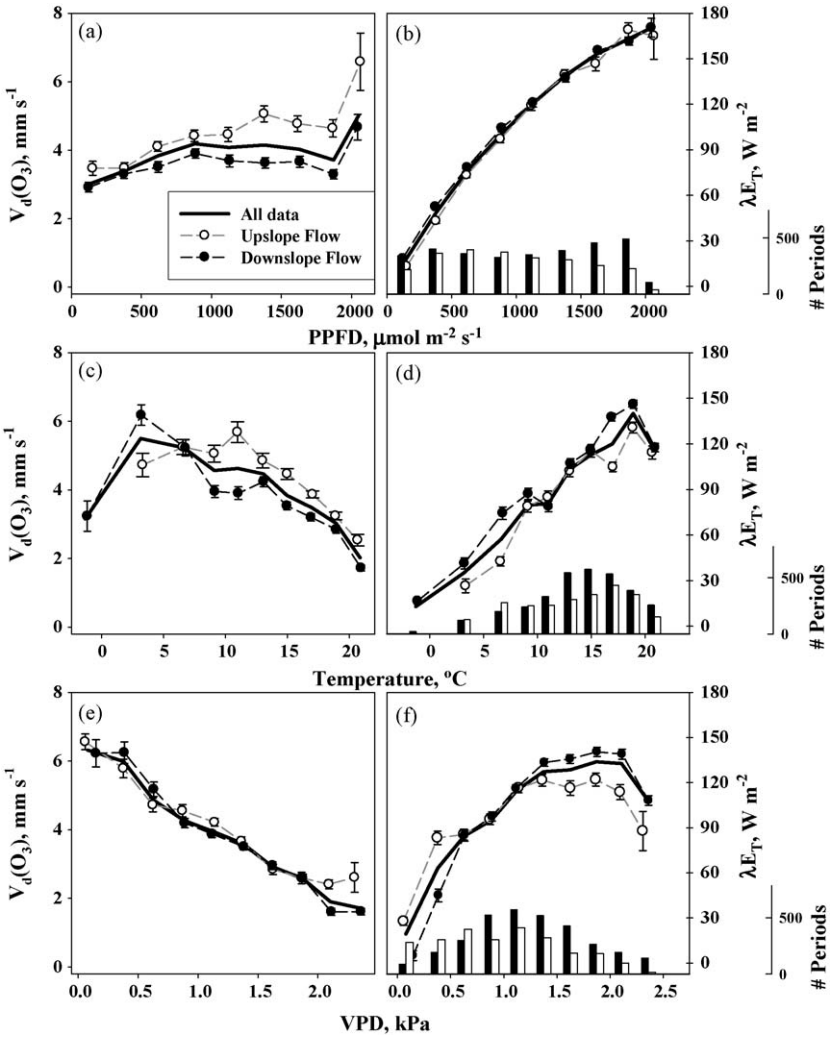

Fig. 4. Plots of median daytime O_3 deposition velocity (V_d) and transpiration flux (λE_T) binned as a function of above-canopy PPFD (a and b), air temperature (c and d) and VPD (e and f). White (upslope) and black (downslope) barplots on (b), (d) and (f) indicate the number (#) of flux periods in each bin. Errors bars on all plots are the standard error ($\sigma/N^{1/2}$).

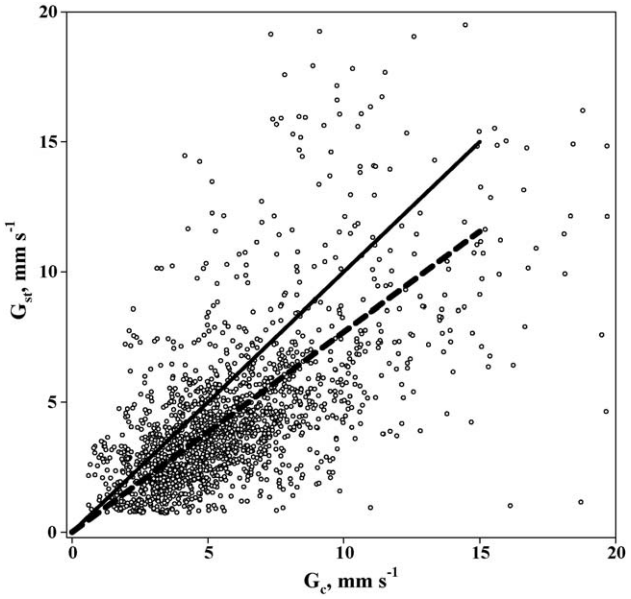

Fig. 5. Plot of daytime O_3 G_{st} vs. G_c for the 2005 growing season data. The solid line drawn is the 1:1 line (indicating O_3 uptake is stomatal only) and the dashed line indicates a G_{st}/G_c ratio (slope) of 0.80.

of O_3 (G_{st}) vs. the total conductance (G_c) for the 2005 measurement period. The ratio of G_{st}/G_c was, on average, less than unity suggesting non-stomatal depositional pathways. The summertime, daytime stomatal contribution to the flux averaged $81 \pm 2\%$ (Table 2), which is consistent with previously reported values (Lamaud et al., 2002; Cieslik, 2004).

The temperature at the roughness length for heat, $T(z'_0)$, can also be estimated through a resistance model analogous to Eq. (11) using the sensible heat flux, H (Gerosa et al., 2007):

$$T(z'_0) = T_{z=21\,\mathrm{m}} + \frac{(R_a + R_b)H}{\rho c_p}. \quad (13)$$

where R_b in this instance is the laminar sublayer resistance for heat. Eq. (13) tended to give leaf temperatures that were ~2–4 °C above the measured within-canopy air temperature. When $T(z'_0)$ derived from Eq. (13) was used to calculate G_{st} from Eq. (11), it led to a smaller stomatal partitioning ($59 \pm 2\%$, standard error). This indicates the sensitivity of $e_{sat}(T(z'_0))$ to the leaf temperature used. As the morphology of conifer needles facilitates the rapid dissipation of excess heat to the surrounding air, this large temperature difference seemed unlikely. Gerosa et al. (2007) also noted that using the sensible heat flux to obtain $T(z'_0)$ over an onion field led to slightly higher leaf temperatures than measured directly. They postulated that cooling from evaporation was likely responsible for the bias.

Gerosa et al. (2007) showed that using ambient within-canopy temperature to calculate stomatal ozone flux agreed very well with those calculated using measured leaf temperatures; yet they recommended using the sensible heat flux to determine leaf temperatures since it had less sensitivity to measurement errors. However, measurement errors in ambient air temperatures are typically much smaller than errors in flux measurements (especially in non-ideal terrain where advection can be significant), which is why we preferred to rely on a measured environmental scalar (e.g., temperature), rather than the calculated sensible heat flux. It should also be noted that $e(z'_0)$ (see Eq. (11)) was determined by both using within-canopy humidity and by a resistance model for water vapor flux analogous to Eq. (13) for $T(z'_0)$. Both of these methods for $e(z'_0)$ gave nearly equivalent G_{st}/G_c partitioning (0.76 ± 0.02, using $RH_{z=8\,m}$, and 0.81 ± 0.02, using the resistance model, Table 2). This is due to the small water vapor gradients observed and the lower sensitivity of the calculations to $e(z'_0)$ as compared with $T(z'_0)$.

Use of the inverted Penman–Monteith equation (Eq. (12)) gave nearly identical results to the ER method (assuming $T_{8\,m} = T(z'_0)$). Daytime median G_{st}/G_c ratios of 0.79 ± 0.02 (standard error) were found using all of the data. Ratios computed for individual years/seasons were also consistent when calculated for both methods. However, we did observe differences in these two methods when looking at trends with different environmental drivers. These are small differences that only become statistically significant due to the large data set used for this analysis.

Fig. 6 shows the derived G_{st} and G_{ns} for O_3 as functions of PPFD, temperature and VPD by both the ER and PM methods. The PPFD dependencies predicted by the ER method are consistent with the transpiration flux and $V_d(O_3)$ data (Fig. 4); higher G_{st} during upslope flows (Fig. 4f, Table 2) due to greater stomatal conductance, which is, in turn, driven by the higher humidity observed. However, the PM model predicts nearly equivalent G_{st} for both upslope and downslope flows. This results in a distinct upslope/downslope bias in the non-stomatal contribution to the flux. Regardless of the mechanism of non-stomatal deposition (including gas phase chemistry), the behavior of the PM model seems difficult to reconcile without invoking major changes in forest characteristics from east to west. Conversely the Evaporation/Resistance method predicts identical G_{ns} regardless of wind direction. At the highest PPFD levels, an increase in G_{ns} was observed from both the ER and PM methods; however, over most of the range (<1700 μmol m^{-2} s^{-1}) both models predict a decreasing behavior of G_{ns} (except for the PM model for upslope conditions which appears to be light independent). It is possible that within-canopy photochemistry, driven by the high photon fluxes and associated high air temperatures (with high hydrocarbon emission rates from the trees) drives a larger loss of O_3 at the highest PPFD levels.

The temperature dependency of G_{st} using the ER method follows trends similar to those of the O_3 deposition velocity (Figs. 4c and 6c). Between 7.5 and 16 °C, larger G_{st} are predicted during upslope flow as expected due to the higher humidity during these periods. However, the PM method shows no clear wind direction dependence for G_{st}. As a result, G_{ns} predicted by the PM method is markedly different for upslope and downslope flows, again requiring us to invoke a wind direction bias in the non-stomatal component of the flux (Fig. 6d). Finally, both models predict decreasing G_{st} with VPD as expected, but again, the PM model predicts an upslope/downslope bias in the variation of G_{st} and G_{ns}.

From this analysis, we conclude that one must use caution in the selection of a stomatal conductance model as the PM model appears to lead to biases in the behavior of the flux components that are difficult to explain. The cause of this appears to be within the resistances derived for turbulent transport (R_a) and diffusion across the laminar sublayer (R_b). Since models of both R_a and R_b are dependent on the inverse of the friction velocity (u^*), the lower wind speeds and u^* observed during typical upslope events led to larger values of R_a and R_b. In total magnitude, these differences are small (≤10 s m^{-1}), so that in summation (for example, Eqs. (6) or (11)), R_T (=R_a + R_b) is a small term relative to the total stomatal or surface resistance and this behavior is of little consequence. However, in Eq. (12) it is used to relate the energy balance measured at z = 21 m to the leaf surface and appears as a multiplicative term. In this fashion, the wind direction tendencies of R_T are expressed and somewhat amplified by errors in the surface energy budget. Our past work at this site has shown that the residual gap left over after closure of the surface energy balance is around 15–20% (Turnipseed et al., 2002), leading to an

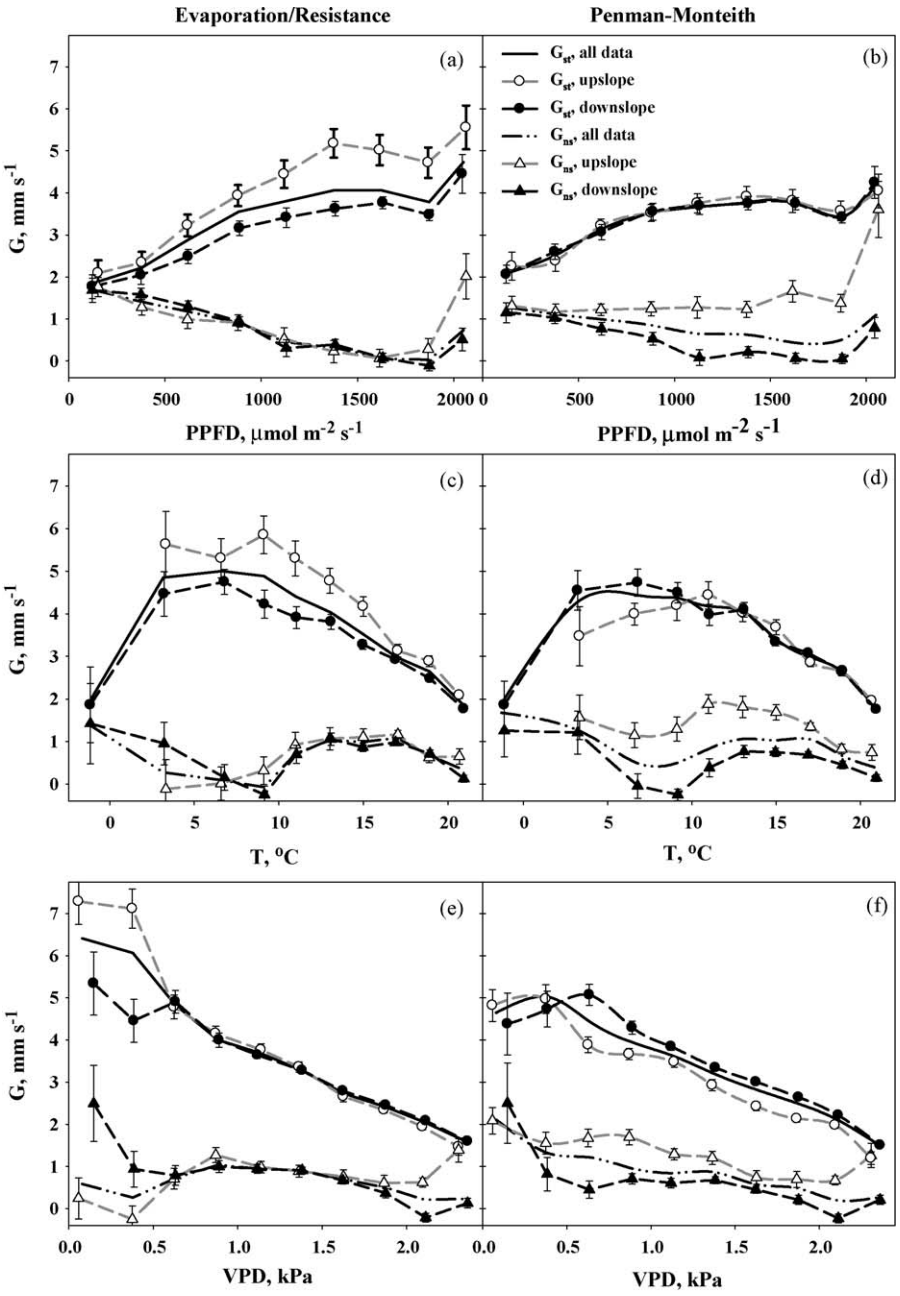

Fig. 6. Plots of binned median daytime G_{st} (circles) and G_{ns} (triangles) vs. above-canopy PPFD (a and b), temperature (c and d), and VPD (e and f). Plots (a), (c) and (e) use the Evaporation/Resistance model (Eq. (11)), plots (b), (d) and (f) use the Penman–Monteith method (Eq. (12)) to derive the stomatal conductance.

overestimate of the energy balance term in Eq. (12). As VPD is typically smaller during upslope periods, larger upslope resistances in the energy balance term of Eq. (12) tend to offset the expected behavior of stomatal conductance with VPD (see Fig. 6b and d). Our calculations using the ER method (with $T_{z=8\,m} = T(z'_0)$) are more consistent with VPD variability being the primary driving force behind stomatal conductance as expected from previous studies (Jarvis, 1976).

Further insight into these resistances to mass transfer (R_T) can be found by using measured temperature gradients and Eq. (13). Daytime sensible heat fluxes showed no statistical differences between upslope and downslope airflow as a function of incident radiation. Daytime temperature gradients between 21 and 8 m also tended to show no upslope/downslope differences until high PPFD values (>1200 μmol m^{-2} s^{-1}) where ΔT (=$T_{z=8\,m} - T_{z=21\,m}$) was actually slightly smaller for upslope flow (data not shown). Via Eq. (13), this implies that R_T (and likely, R_a) for upslopes should be equivalent or less than those during downslope flows, converse to what is predicted by the typical formulations (Garland, 1977; Hicks et al., 1987) used here. It is likely that these formulations (which were derived for the surface layer over flat surfaces), including stability functions (Dyer, 1974), may not adequately describe mass transport in the roughness sublayer over a tall rough canopy. We also suspect that this may also play a role in the higher leaf temperatures derived via Eq. (13). This lends more support to our preference of the ER method using measured environmental variables within the canopy.

The ratio of the median G_{st} to G_c (data from Fig. 6) varied between 0.6 and 1, with the variation due primarily to changes in G_{st} as opposed to a changing G_{ns} (Fig. 6). G_{ns} reaches its largest fractional uptake at either low light levels or high temperatures and VPD. These conditions are typified by low plant activity,

limited either by low radiation or by water constraints during hot, dry periods (Monson et al., 2002). However, under these same conditions, the non-stomatal flux contribution either remains unchanged or perhaps increases slightly. The variations of plant stomatal conductance with PPFD, T and VPD and the impact on ozone deposition has been well studied; however, very few studies have looked at the effect of these environmental drivers on the non-stomatal component of the flux. Past studies have reported that G_{ns} exhibits a diel behavior (Rondón et al., 1993; Granat and Richter, 1995; Coe et al., 1995; Gerosa et al., 2003; Hogg et al., 2007) reaching a maximum during midday periods. However, the covariance of PPFD and temperature has made it difficult to determine whether this trend is driven by temperature (Fowler et al., 2001; Kurpius and Goldstein, 2003), PPFD (Rondón et al., 1993; Coe et al., 1995), or some combination of the two. The study of Hogg et al. (2007) is the only study to show independent responses of G_{ns} for both PPFD and temperature.

In our results it appears that G_{ns} decreased with PPFD over most of the range. This is contrary to the study of Hogg et al. (2007), who observed a steady increase of G_{ns} with PPFD, suggesting either a photochemical loss of O_3 at the surfaces or a photolytically driven biological process that interacts with O_3. We only see some evidence of this at high PPFD levels where an increase in G_{ns} was observed. As mentioned above, this may be indicative of within-canopy photochemistry driving a larger loss of O_3 and bears further study. There also appears to be no clear trend in G_{ns} with VPD. The large variations in G_{ns} (and G_{st}) which occur at low VPD (<0.5 kPa) likely reflect the difficulties (and associated higher measurement errors) of determining G_{st} at low VPD since the difficulties of accurately partitioning λE_T from evaporative water flux are magnified. G_{ns} tends to show a slight increase with temperature between 8 °C (where $G_{ns} \sim 0$) and 13 °C, but then levels off and remains nearly constant at higher temperatures. The increase in G_{ns} at low temperature (<5 °C) must be viewed with caution as the amount of growing season data in this temperature range is sparse (<2% of the total data set) and it is unclear whether models designed to predict G_{st} are robust at these low temperatures. Fowler et al. (2001), Mikkelsen et al. (2004) and Kurpius and Goldstein (2003) have all observed steady increases in G_{ns} with temperature. This has been attributed to either thermal decomposition of O_3 (Fowler et al., 2001) or rapid chemical reactions with other trace species (such as NO or hydrocarbons) either on the plant surfaces (Fruekilde et al., 1998) or that are emitted (Mikkelsen et al., 2004; Kurpius and Goldstein, 2003). Our data is more similar to that reported by Hogg et al. (2007), who observed an increase in G_{ns} that reached a maximum at ~22–25 °C, followed by a decrease at higher temperatures. These authors suggested some form of biological process with an optimum temperature to explain their observations; however, the identification of this process remains speculative. As also noted by Hogg et al. (2007), these observations are inconsistent with simple thermal decomposition of ozone on surfaces.

3.4. Wetness effects and nocturnal O_3 uptake

Unexpectedly large O_3 deposition fluxes were sometimes observed during late afternoon upslope periods; we determined that these large fluxes often followed precipitation events. Massman (2004) has presented a synopsis of past studies concerning surface wetness and O_3 deposition, and noted that the presence of surface wetness often (but not always) tends to increase O_3 uptake (e.g., Fuentes et al., 1992; Grantz et al., 1995; Pleijel et al., 1995; Lamaud et al., 2002; Zhang et al., 2002). This is surprising in light of the low solubility of O_3. Chamber studies by Fuentes et al. (1993) indicated that the effect of surface wetness was species-dependent, reporting increases in O_3 uptake with wetness for a hypostomatous red maple and decreases for a hybrid amphistomatous poplar. Altimir et al. (2006) recently presented a study indicating that wetness effects are a dominant driver of the non-stomatal flux at a relatively moist boreal forest site. In general, the wetness effects on total O_3 uptake represent a balance between various stomatal effects (physical stomatal blockage, lowering of VPD) and apparent enhancements of the non-stomatal flux (Altimir et al., 2006).

In analyzing the wetness effects on O_3 deposition, we have only looked at the variations in the total conductance (G_c), as models which predict stomatal conductance are not valid during wet conditions (Monteith and Unsworth, 1990). The wetness effects on O_3 deposition at the Niwot Ridge site is somewhat simplified by the fact that dew formation is virtually nonexistent. Consistent nocturnal drainage winds tend to dry the canopy at night and do not allow a build-up of H_2O vapor within the canopy from soil evaporation ($RH_{z=8\,m} > 95\%$ only 2.8% of the nighttime periods). Therefore wetness effects are primarily due to precipitation. We can again take advantage of the meteorology at Niwot Ridge where convective thunderstorm activity sometimes accompanies afternoon upslope flows. When we restricted our data analysis to days with precipitation (>5 mm) during the hours between 12:00 and 16:00 local time, the surface conductance (G_c) was significantly higher following afternoon precipitation events and remained between 1.5 and 3 times larger through the nighttime hours, compared to dry days (Fig. 7). It was observed that, on average, nocturnal G_c increased from 1.9 to 5.4 mm s^{-1} following afternoon precipitation events. From the diel trends shown in Fig. 7, it

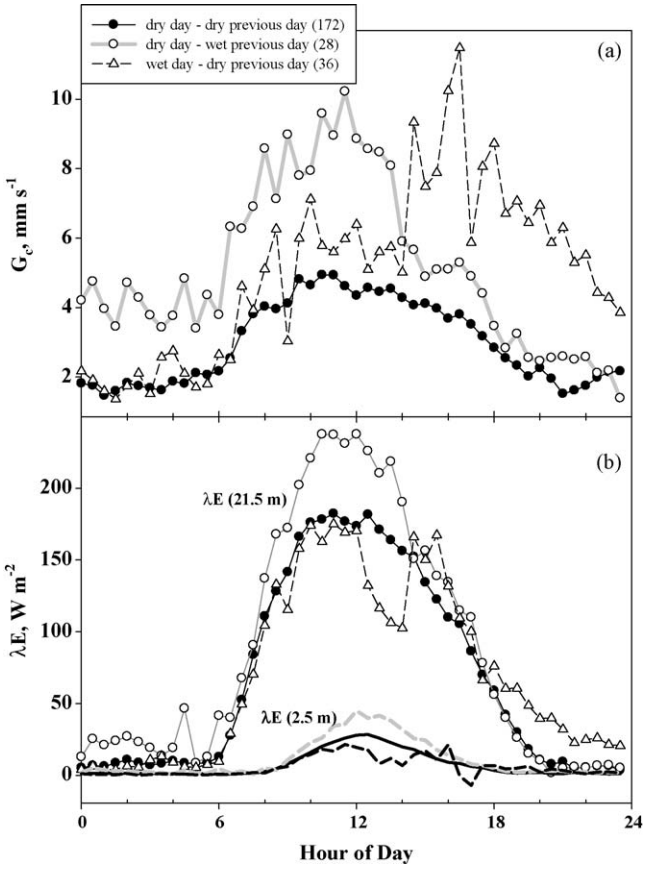

Fig. 7. (a) Average diel profiles of O_3 surface conductance, G_c and (b) latent heat fluxes above (21.5 m) and below (2.5 m) the canopy during days with varying precipitation. Black circles/solid lines = dry day with dry previous day (172 days averaged), white circles/gray lines = dry day with precipitation (>5 mm) on previous day (36 days), and white triangles/black dashed lines = dry previous day with precipitation (>5 mm) between 12:00 and 16:00 local time (28 days).

appears that this enhancement lasted through the night following precipitation, but was not present the following night (after a dry day). One further note of interest is that daytime fluxes on days following precipitation (after the leaf surfaces have dried) increased along with increases in water vapor fluxes. Although $\lambda E_{z=2.5\ m}$ does increase (suggesting larger soil evaporation), the latent heat flux difference ($\lambda E_{z=21.5\ m} - \lambda E_{z=2.5\ m}$) increases by a much larger amount, suggesting higher transpiration rates (Fig. 7b) after replenishment of the soil water reserves; thus, it appears that both G_{st} and G_{ns} were enhanced following precipitation, but with differing time responses.

At the present time, we do not fully understand the nature of the enhanced O_3 uptake immediately following rain events. Altimir et al. (2006) discussed the possibilities of either (1) chemical reactions of O_3 that are modulated by water films on the surface, (2) incomplete closure of plant stomates during nocturnal hours when leaves were wet and (3) enhanced reactive hydrocarbon emissions which can subsequently react with O_3. There is some evidence from this study to support all three of these hypotheses. Fig. 8a shows plots of the observed nocturnal G_c (PPFD < 15 mmol m^{-2} s^{-1}, $u^* > 0.2$ m s^{-1}) vs. the measured relative humidity. Even though the majority of data occurs under "dry" conditions (RH $< 65\%$), the variability of G_c with relative humidity is similar to that reported by Altimir et al. (2004), showing a strong increase when RH > 60–70%. Previous studies have shown that liquid water films form on the surfaces of leaves and needles when RH $> 70\%$ (Burkhardt and Eiden, 1994; Altimir et al., 2006). Although the presence of water films was not directly measured in this study, the strong increase in G_c at high humidity lends support to their importance toward O_3 deposition.

Nighttime G_c binned as a function of temperature under typical dry conditions (RH $< 65\%$) are shown in the inset of Fig. 8a. Nocturnal G_c tends to decrease with increasing temperature. This is contrary to the study by Mikkelsen et al. (2004), who showed increasing nighttime O_3 deposition with temperature in a spruce forest, regardless of season. They suggested that reactions with NO and volatile organics (VOCs) may be responsible for their observed temperature dependence. These contributions would be expected to be small at the Niwot Ridge site due to low emission rates of VOCs (Rinne et al., 2000; Karl et al., 2002) and the nocturnal atmospheric structure (high stability within the canopy and associated drainage flows, Yi et al., 2005) which effectively decouples within-canopy airflows (which may be impacted by O_3-reactive species like NO) from that above the canopy where O_3 fluxes were measured.

However, we do observe that nocturnal G_c tends to vary with the latent heat flux above the canopy (Fig. 8b) up to values of about 75 W m^{-2}. It is typically assumed that nighttime latent heat flux is due solely to evaporation; however, recent studies have shown that most trees actually do experience nighttime transpiration (Dawson et al., 2007; Fisher et al., 2007). Dawson et al. (2007) have shown that nocturnal transpiration is strongly tied to available soil water. In relatively dry ecosystems (similar to Niwot Ridge), they found stronger nocturnal transpiration following rain events. Although nighttime λE is a measure of both evaporation and transpiration, decoupling of within and above-canopy flows tends to limit influences from the soil surface and lower canopy where most of the evaporation occurs. Sap flow measurements conducted

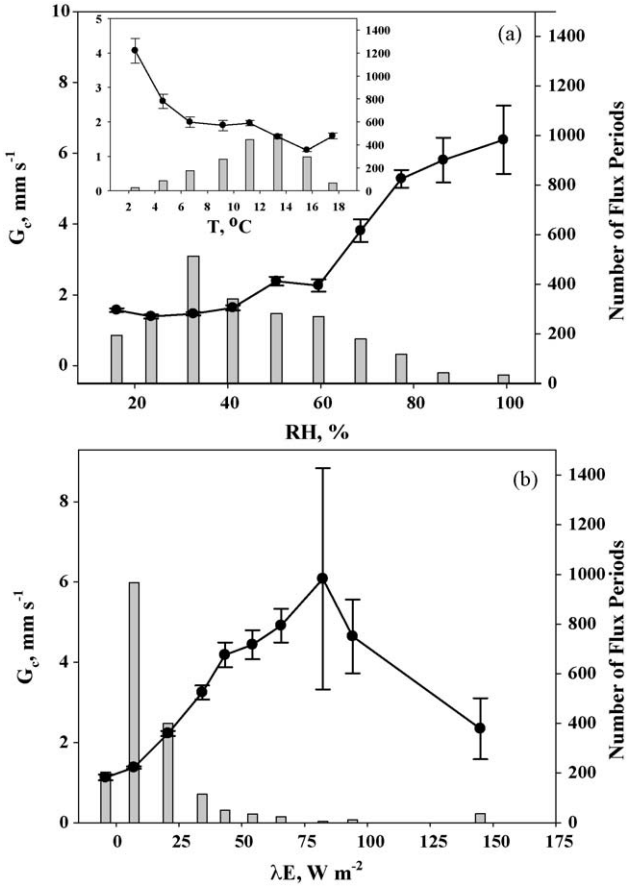

Fig. 8. Plot of the binned nocturnal O_3 surface conductance, G_c vs. (a) relative humidity and (b) latent heat fluxes with RH $< 65\%$. Bars denote the number of flux periods within each bin. Error bars are the standard error. The inset in (a) shows the relationship of nocturnal G_c with temperature for RH $< 65\%$.

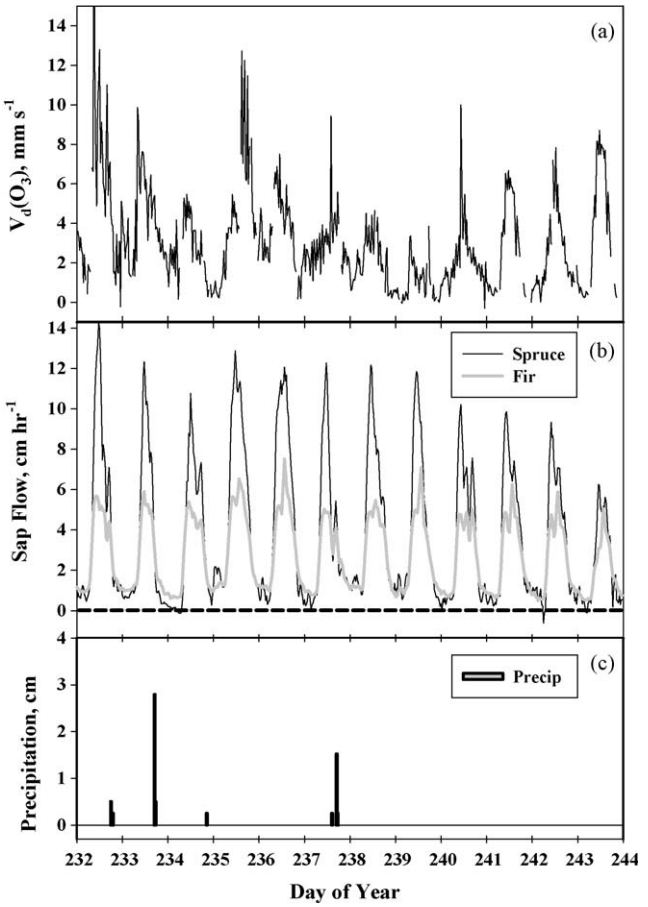

Fig. 9. Time series of (a) $V_d(O_3)$, (b) measured sap flow in Engelmann spruce and subalpine fir and (c) precipitation during 12 days of August, 2005.

at Niwot Ridge in August of 2005 indicated nonzero sap flow in all three conifer species with nearly 15% of the total sap flow occurring during nighttime hours. An example of the August data is shown in Fig. 9. Nonzero sap flow occurred on two thirds of the nights in this month, and, following the criteria relating nocturnal transpiration to VPD described by Dawson et al. (2007), most of these appeared to be the result of nocturnal transpiration (as opposed to xylem refilling). Although there were nights showing both elevated sap flow and ozone deposition (for example, Fig. 9, DOY = 238), the overall correlation for this month between nocturnal sap flow with either G_c or λE was relatively poor. This is likely due to the relatively small data set and the complication of inadequate nocturnal turbulence affecting the flux measurements. However, the relationship of nocturnal G_c with λE (Fig. 8b) and the enhancement of G_c after rainfall (Figs. 7 and 9) may be suggestive of a causative relationship between nighttime stomatal opening and O_3 flux. Such a relationship may be important as often plant biochemical detoxification mechanisms are down-regulated at night, making the plants more susceptible to nighttime O_3 damage (Matyssek et al., 1995; Musselman and Minnick, 2000).

The final mechanism that may explain the higher $V_d(O_3)$ following precipitation events involves the enhanced emission of volatile hydrocarbons as a reactive sink for O_3. The premise of open stomates at night does not discount this mechanism as the stomates are often pathways for these compounds to be released to the atmosphere. Preliminary measurements suggest that fluxes of monoterpenes are enhanced by nearly a factor of 5 following a strong thunderstorm (which included hail) at this site (Turnipseed, unpublished results). However, it is not known whether this enhancement occurs following smaller, less intense, rain events, as the observed emission increase could be due to physical damage from the hail to the vegetation. The duration of this emission enhancement is also not currently known. Furthermore, VOCs which could react rapidly enough with O_3 to affect the measured flux were not detected in the ambient air at that time.

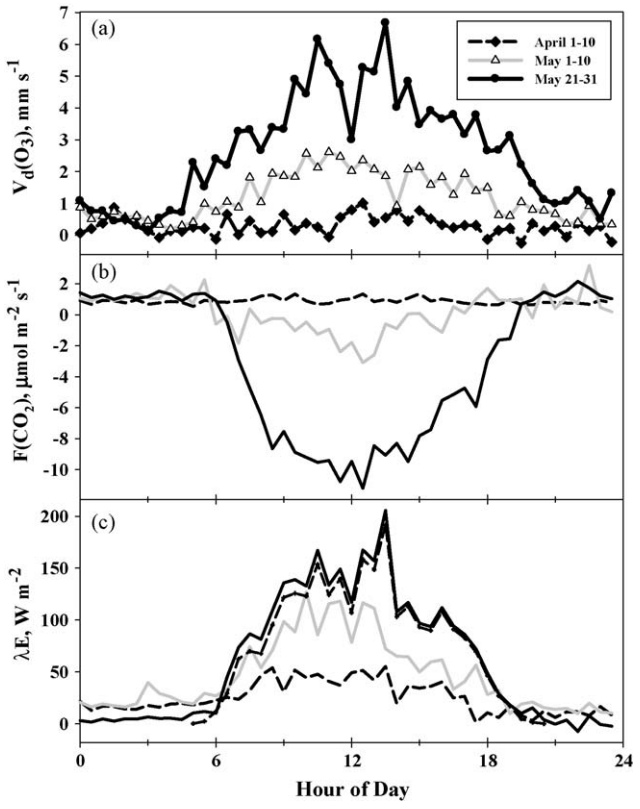

Fig. 10. Average 10-day diel cycles during the spring of 2005 showing (a) O_3 deposition velocity, (b) $F(CO_2)$ and (c) latent heat flux, λE. The thin dashed line with points in (c) shows the modeled λE_T for the May 21–31 period.

3.5. Transition season fluxes

Spring and fall represent transition periods in the ecosystem carbon balance from either CO_2 loss to accumulation (spring turn-on) or vice versa (fall shutdown). Fig. 10 shows diurnal patterns of CO_2 flux, λE and $V_d(O_3)$ during the spring turn-on of 2005. O_3 deposition is tightly correlated with $F(CO_2)$ and λE, again showing the importance of springtime opening of plant stomates on the O_3 flux. This linkage to stomatal uptake was especially true during the autumn seasons that are relatively dry. From stomatal conductance estimates using the ER method, it appeared that stomatal uptake of O_3 accounted for nearly all of the measured deposition during these periods (data not shown).

In springtime, separation of G_{st} and G_{ns} is complicated by the interception of snow by the canopy and subsequent sublimation or evaporation. During mid- and early-spring periods, the modeled stomatal O_3 flux (based on λE_T fluxes) is often larger than the total measured O_3 flux. A previous study at this site (Molotch et al., 2007) indicated that only 37% of the total observed wintertime sublimation originated at the ground surface snowpack. The remainder was assumed to be due to sublimation of snow intercepted by the canopy. Even though melting and evaporation also play a role during the spring (in contrast to the Molotch et al., 2007 study), the large amount of spring snowfall observed during this study (average precipitation of 160 mm Snow Water Equivalent from April to mid-May) suggest that canopy snow interception must be accounted for in order to properly determine the stomatal component of the flux. Although the model logic of SIPNET includes an explicit attempt to estimate snow sublimation within its partitioning of water fluxes, it is only roughly parameterized. Furthermore, the difference in λE with height (at 21.5 and 2.5 m) would include canopy sublimation/evaporation as transpiration. At the end of the spring season, when snow interception was insignificant (i.e., no further snowfall) and the trees were fully active, the stomatal fraction of the flux behaved similarly to summertime fluxes (as described in the previous section).

3.6. Non-growing season flux measurements

Wintertime O_3 fluxes were small, with corresponding $V_d(O_3)$ averaging only about 0.7 mm s^{-1}. Since the forest is photosynthetically inactive during these periods, we assume that this represents only non-stomatal uptake of O_3. There was no statistical difference observed between measurements during the different years. These measurements were similar in magnitude to most previous measurements over snow-covered surfaces (Munger et al., 1996; Helmig et al., 2007); however, it should be noted that although there was constant snow coverage over soils during these measurements (~1 m depth), vegetation foliage and branches were typically uncovered and this could have led to larger estimated deposition rates than might have occurred on the snow surface alone.

$V_d(O_3)$ still exhibited a small diurnal trend with nighttime values near 0.5 mm s^{-1} and midday values reaching nearly 1.2 mm s^{-1}. There was no clear dependence of $V_d(O_3)$ on the major environmental drivers (PPFD, temperature, humidity) and much of the observed diurnal trend can be explained by changes in turbulence. When binned as a function of λE, there appeared to be a distinct dependence of $V_d(O_3)$ on the latent heat flux (Fig. 11), although there was substantially less data at $\lambda E > 45$ W m^{-2} with considerably more scatter. Monson et al. (2005) noted small isolated bursts of carbon uptake at this site during late winter (March) which would imply partial stomatal opening. However, these were sporadic and short-lived. In general, wintertime λE at

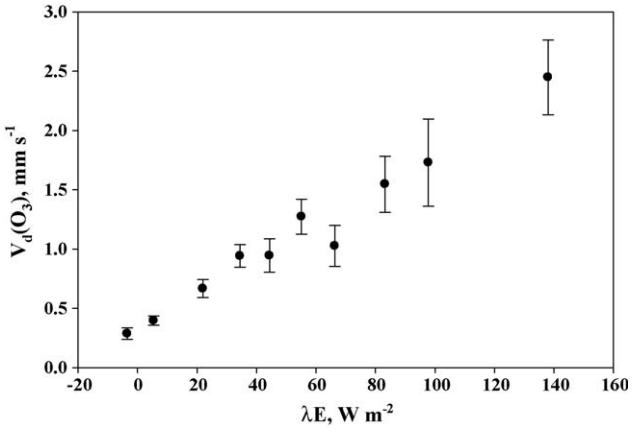

Fig. 11. Plot of the median wintertime deposition velocity for O_3 binned as a function of latent heat flux. Error bars are the standard error.

this site tends to be tied more to precipitation events (Turnipseed et al., 2002; Molotch et al., 2007), and is largely due to sublimation of canopy-intercepted snow (Molotch et al., 2007). For periods during or immediately following precipitation events, $V_d(O_3)$ increased to 1.3–1.4 mm s^{-1}, compared to the average of 0.6–0.7 mm s^{-1}; this suggests that precipitation (whether liquid or, more likely, frozen) tends to modify the O_3 surface sink. This linkage between wintertime precipitation and O_3 fluxes has also been noted by Altimir et al. (2006). Whether this enhancement suggests slight stomatal opening during the winter season, an increased reactive cuticular surface, or interactions with the intercepted snow within the canopy, remains unclear.

4. Conclusions

In the present study we investigated the seasonal controls over and variability of O_3 deposition at a high elevation subalpine forest that experiences periodic episodes of anthropogenic pollution. The mountain–valley wind system and the distance from the Denver metropolitan area at this site create peak O_3 concentrations in the late afternoon/early evening, after the peak in vegetative stomatal conductance. The flux of O_3 shows a diurnal peak which is intermediate between those of CO_2 uptake and O_3 concentration. The temporal offset between peak photosynthetic activity and peak O_3 concentration lessens the potential for deleterious effects from O_3 uptake.

After PPFD (which drives plant activity), environmental conditions during different flow regimes indicated VPD was likely the most dominant environmental driver controlling the daytime deposition of O_3 at this site through its influence over stomatal conductance. From comparisons with other studies in similar forests (Zeller and Nikolov, 2000), it was not surprising that ~80% of daytime O_3 uptake was observed to be taken up into the vegetation via stomata. Two separate methods (Evaporative/Resistance and Penman–Monteith) were used to estimate the stomatal fraction of O_3 uptake with reasonable agreement. However, the two models differed in how they represented variation of the stomatal component with the primary environmental drivers (PPFD, temperature, VPD). In general, the Evaporative/Resistance method was more consistent with the observed environmental conditions and the expected stomatal responses of the forest. The results showed that the stomatal fraction of O_3 uptake decreased at high VPD and temperatures, leading to a higher non-stomatal fraction under these conditions. Our observed temperature dependence of G_{ns} is inconsistent with simple thermal decomposition, but does not exclude past hypotheses concerning surface reactions or reactions with emitted reactive compounds.

Surface wetness appeared to play an important role in O_3 deposition. During the growing season, surface conductance (G_c) to O_3 increased after midday precipitation events and continued at an elevated level throughout the night. Nocturnal deposition velocities for O_3 were well correlated with latent heat fluxes suggesting that stomata remained open at night and caused the increased O_3 flux. This has implications for plant health as it is possible that detoxification mechanisms within the plants may be down-regulated at night, leaving them more susceptible to damage from atmospheric oxidants. Further studies are necessary to elucidate the link between O_3 deposition and nocturnal stomatal conductance. $V_d(O_3)$ showed a consistent dependency on latent heat fluxes during the winter as well. As wintertime latent heat fluxes have been shown to be tied to precipitation events, this leads to a role for precipitation in wintertime ozone deposition as well. The exact mechanism of this enhancement in the O_3 fluxes is uncertain and merits further study.

Acknowledgements

The National Center for Atmospheric Research is operated by the University Corporation for Atmospheric Research under the sponsorship of the National Science Foundation. These studies were supported in part by a grant from the Western Section of the National Institute for Climate Change Research (NICCR), which is funded by the Office of Biological and Environmental Research (BER) in the U.S. Department of Energy. Andrew Turnipseed would like to thank Tony Delany (retired from NCAR), Dave Bowling (University of Utah) and Steve Hoskins for assistance in the early stages of this project.

References

Altimir, N., Kolari, P., Tuovinen, J.P., Vesala, T., Bäck, J., Suni, T., Kulmala, M., Hari, P., 2006. Foliage surface ozone deposition: a role for surface moisture? Biogeosciences 3, 209–228.

Altimir, N., Tuovinen, J.P., Vesala, T., Kulmala, M., Hari, P., 2004. Measurements of ozone removal by Scots pine shoots: calibration of a stomatal uptake model including the nonstomatal part. Atmospheric Environment 38, 2387–2398.

Brazel, A.J., Brazel, S.W., 1983. Summer Diurnal wind patterns at 3000 m surface level, Front Range, Colorado, USA. Physical Geography 4 (1), 53–61.

Büker, P., Emberson, L.D., Ashmore, M.R., Cambridge, H.M., Jacobs, C.M.J., Massman, W.J., Müller, J., Nikolov, N., Novak, K., Oksanen, E., Schaub, M., de la Torre, D., 2007. Comparison of different stomatal conductance algorithms for ozone flux modeling. Environmental Pollution 146, 726–735.

Burgess, S.S.O., Adams, M.A., Turner, N.C., Beverly, C.R., Ong, C.K., Khan, A.A.H., Bleby, T.M., 2001. An improved heat pulse method to measure low and reverse rates of sap flow in woody plants. Tree Physiology 21, 589–598.

Burkhardt, J., Eiden, R., 1994. Thin water films on coniferous needles. Atmospheric Environment 28, 2001–2017.

Bytnerowicz, A., Musselman, R., Szaro, R., 2004. Introduction: effects of air pollution on the Central and Eastern European mountain forests. Environmental Pollution 130, 1–3.

Chappelka, A.H., Samuelson, L.J., 1998. Ambient ozone effects on forest trees of the Eastern United States: a review. New Phytologist 139 (1), 91–108.

Cieslik, S.A., 2004. Ozone uptake by various surface types: a comparison between dose and exposure. Atmospheric Environment 38, 2409–2420.

Coe, H., Gallagher, M.W., Choularton, T.W., Dore, C., 1995. Canopy scale measurements of stomatal and cuticular O_3 uptake by Sitka spruce. Atmospheric Environment 29, 1413–1423.

Curtis, L., Rea, W., Smith-Willis, P., Fenyves, E., Pan, Y., 2006. Adverse health effects of outdoor air pollutants. Environment International 32, 815–830.

Dawson, T.E., Burgess, S.S.O., Tu, K.P., Oliveira, R.S., Santiago, L.S., Fisher, J.B., Simonin, K.A., Ambrose, A.R., 2007. Nighttime transpiration in woody plants from contrasting ecosystems. Tree Physiology 27, 561–575.

Dyer, A.J., 1974. A review of flux–profile relationships. Boundary Layer Meteorology 7, 363–372.

Emberson, L.D., Büker, P., Ashmore, M.R., 2007. Assessing the risk caused by ground level ozone to European forest trees: a case study in pine, beech and oak across different climate regions. Environmental Pollution 147, 454–466.

Fehsenfeld, F.C., Bollinger, M.J., Liu, S.C., Parrish, D.D., McFarland, M., Trainer, M., Kely, D., Murphy, P.C., Albritton, D.L., 1983. A study of ozone in the Colorado mountains. Journal of Atmospheric Chemistry 1, 87–105.

Fisher, J.B., Baldocchi, D.D., Misson, L., Dawson, T.E., Goldstein, A.H., 2007. What the towers don't see at night: nocturnal sap flow in trees and shrubs at two Ameriflux sites in California. Tree Physiology 27, 597–610.

Foken, T., Wichura, B., 1996. Tools for the quality assessment of surface-based flux measurements. Agriculture and Forest Meteorology 78, 83–105.
Fowler, D., Flechard, C., Cape, J.N., Storeton-West, R.L., Coyle, M., 2001. Measurements of ozone deposition to vegetation: quantifying the flux, the stomatal and non-stomatal components. Water, Air, and Soil, Pollution 130, 63–74.
Fruekilde, P., Hjorth, J.N.R., Kotzias, D., Larsen, B., 1998. Ozonolysis at vegetation surfaces: a source of acetone, 4-oxopentanal, 6-methyl-5-hepten-2-one and geranyl acetone. Atmospheric Environment 32, 1893–1902.
Führer, J., Booker, F., 2003. Ecological issues related to ozone: agricultural issues. Environment International 29, 141–154.
Fuentes, J.D., Gillespie, T.J., Bunce, N.J., 1993. Effects on foliage wetness on the dry deposition of ozone onto Red Maple and Poplar leaves. Water, Air and Soil Pollution 74, 189–210.
Fuentes, J.D., Gillespie, T.J., den Hartog, G., Neumann, H.H., 1992. Ozone deposition onto a deciduous forest during dry and wet conditions. Agricultural and Forest Meteorology 62, 1–18.
Garland, J.A., 1977. The dry deposition of sulphur dioxide to land and water surfaces. Proceedings of the Royal Society London A 354, 245–268.
Gerosa, G., Derghi, F., Cieslik, S., 2007. Comparison of different algorithms for stomatal ozone flux determination from micrometeorological measurements. Water, Air, and Soil Pollution 179, 309–321, doi:10.1007/s11270-006-9234-7.
Gerosa, G., Cieslik, S., Ballarin-Denti, A., 2003. Micrometeorological determination of time-integrated stomatal ozone fluxes over wheat: a case study in Northern Italy. Atmospheric Environment 37, 777–788.
Granat, L., Richter, A., 1995. Dry deposition to pine of sulphur dioxide and ozone at low concentrations. Atmospheric Environment 29, 1677–1683.
Grantz, D.A., Zhang, X.J., Massman, W.J., Den Hartog, G., Neumann, H.H., Pederson, J.R., 1995. Effects of stomatal conductance and surface wetness on ozone deposition in field-grown grape. Atmospheric Environment 29, 3189–3198.
Güsten, H., Heinrich, G., 1996. On-line measurements of ozone surface fluxes. Part I. Methodology and instrumentation. Atmospheric Environment 30, 897–909.
Güsten, H., Heinrich, G., Schmidt, R.W.H., Schurath, U., 1992. A novel ozone sensor for direct eddy flux measurements. Journal of Atmospheric Chemistry 14, 73–84.
Heck, W.W., Cure, W.W., Rawlings, J.O., Zaragoza, L.J., Heagle, A.S., Heggestad, H.E., Kohut, R.J., Kress, L.W., Temple, P.J., 1984. Assessing impacts of ozone on agricultural crops: crop yield functions and alternative exposure statistics. Journal of the Air Pollution Control Association 34, 810–817.
Helmig, D., Ganzeveld, L., Butler, T., Oltmans, S.J., 2007. The role of ozone atmosphere-snow gas exchange on polar, boundary-layer tropospheric ozone—a review and sensitivity analysis. Atmospheric Chemistry and Physics 7, 15–30.
Hicks, B.B., Baldocchi, D.D., Meyers, T.P., Hosker, R.P., Matt, D.R., 1987. A preliminary multiple resistance routine for deriving dry deposition velocities from measured quantities. Water, Air, and Soil Pollution 36, 311–330.
Hogg, A., Uddling, J., Ellsworth, D., Carroll, M.A., Pressley, S., Lamb, B., Vogel, C., 2007. Stomatal and non-stomatal fluxes of ozone to a northern mixed hardwood forest. Tellus 59B, 514–525.
Huxman, T.E., Turnipseed, A.A., Sparks, J.P., Harley, P.C., Monson, R.K., 2003. Temperature as a control over ecosystem CO_2 fluxes in a high-elevation, subalpine forest. Oecologia 134, 537–546.
Jacobson, J.S., 1982. Ozone and the growth and productivity of agricultural crops. In: Unsworth, M.H., Ormrod, D.P. (Eds.), Effects of Gaseous Air Pollution in Agricultural and Horticulture. Butterworth Scientific, London.
Jarvis, P.G., 1976. The interpretation of the variations in leaf water potential and stomatal conductance found in canopies in the field. Philosophical Transactions of the Royal Society of London B 273, 593–610.
Karl, T.G., Spirig, C., Prevost, P., Stroud, C., Rinne, J., Greenberg, J., Fall, R., Guenther, A., 2002. Virtual disjunct eddy covariance measurements of organic compounds fluxes from a subalpine forest using proton transfer reaction mass spectrometry. Atmospheric Chemistry and Physics 2, 279–291.
Karlsson, P.E., Uddling, J., Braun, S., Broadmeadow, M., Elvira, S., Gimeno, B.S., Le Thiec, D., Oksanen, E., Vandermeiren, K., Wilkinson, M., Emberson, L.D., 2004. New critical levels for ozone impact on trees based on leaf cumulated ozone uptake. Atmospheric Environment 38, 2283–2294.
Kelliher, F.M., Leuning, R., Schulze, E.-D., 1993. Evaporation and canopy characteristics of coniferous forests and grasslands. Oecologia 95, 153–163.
Kurpius, M., Goldstein, A.H., 2003. Gas-phase chemistry dominates O_3 loss to a forest, implying a source of aerosols and hydroxyl radicals to the atmosphere. Geophysical Research Letters 30, 1371, doi:10.1029/2002GL016785.
Lamaud, E., Carrara, A., Brunet, Y., Lopez, A., Druilhet, A., 2002. Ozone fluxes above and within a pine forest canopy in dry and wet conditions. Atmospheric Environment 36, 77–88.
Losleben, M., Pepin, N., Pedrick, S., 2000. Relationships of precipitation chemistry, atmospheric circulation and elevation at two sites on the Colorado Front Range. Atmospheric Environment 34, 1723–1737.
Massman, W.J., 2004. Toward an ozone standard to protect vegetation based on effective dose: a review of deposition resistances and a possible metric. Atmospheric Environment 38, 2323–2337.
Matyssek, R., Günthardt-Goerg, M., Maurer, S., Keller, T., 1995. Nighttime exposure to ozone reduces whole-plant production in *Betula pendula*. Tree Physiology 15, 159–165.
Mikkelsen, T.N., Ro-Poulsen, H., Hovmand, M.F., Jensen, N.O., Pilegaard, K., Egeløv, A.H., 2004. Five-year measurements of ozone fluxes to a Danish Norway spruce canopy. Atmospheric Environment 38, 2361–2371.
Molotch, N.P., Blanken, P.D., Williams, M.W., Turnipseed, A.A., Monson, R.K., Margulis, S.A., 2007. Estimating sublimation of intercepted and sub-canopy snow using eddy covariance systems. Hydrological Processes 21, 1567–1575.
Monson, R.K., Turnipseed, A.A., Sparks, J.P., Harley, P.C., Scott-Denton, L.E., Sparks, K., Huxman, T.E., 2002. Carbon sequestration in a high-elevation subalpine forest. Global Change Biology 8, 1–20.
Monson, R.K., Sparks, J.P., Rosenstiel, T.N., Scott-Denton, L.E., Huxman, T.E., Harley, P.C., Turnipseed, A.A., Burns, S.P., Backlund, B., Hu, J., 2005. Climatic influences on net ecosystem CO_2 exchange during the transition from wintertime carbon source to springtime carbon sink in a high-elevation, subalpine forest. Oecologia 146, 130–147.
Monteith, J.L., Unsworth, M., 1990. Principles of Environmental Physics, 2nd ed. Arnold, London.
Moore, D., Hu, J., Sacks, W.J., Schimel, D.S., Monson, R.K., 2008. Estimating transpiration and the sensitivity of carbon uptake to water availability in a subalpine forest using a simple ecosystem process model informed by measured net CO_2 and H_2O fluxes. Agricultural and Forest Meteorology 148, 1467–1477.
Munger, J.W., Wofsy, S.C., Bakwin, P.S., Fan, S.M., Goulden, M.L., Baube, B.C., Goldstein, A.H., Moore, K.E., Fitzjarrald, D.R., 1996. Atmospheric deposition of reactive nitrogen oxides and ozone in a temperate deciduous forest and a subarctic woodland. 1. Measurements and mechanisms. Journal of Geophysical Research 101, 12639–12657.
Musselman, R.C., Massman, W.J., 1999. Nocturnal stomatal conductance and ambient air quality standards for ozone. Atmospheric Environment 34, 719–733.
Musselman, R.C., Minnick, T.J., 2000. Nocturnal stomatal conductance and ambient air quality standards for ozone. Atmospheric Environment 34, 719–733.
Parrish, D.D., Trainer, M., Williams, E.J., Fahey, D.W., Hübler, G., Eubank, C.S., Liu, S.C., Murphy, P.C., Albritton, D.L., Fehsenfeld, F.C., 1986a. Measurements of the NOx-O_3 photostationary state at Niwot Ridge, Colorado. Journal of Geophysical Research 91, 5361–5370.
Parrish, D.D., Fahey, D.W., Williams, E.J., Liu, S.C., Trainer, M., Murphy, P.C., Albritton, D.L., Fehsenfeld, F.C., 1986b. Background ozone and anthropogenic ozone enhancement at Niwot Ridge, Colorado. Journal of Atmospheric Chemistry 4, 63–80.
Pleijel, H., Pihl Karlsson, G., Danielsson, H., 1995. Surface wetness enhances ozone deposition to a pasture canopy. Atmospheric Environment 29, 3391–3393.
Pye, J.M., 1988. Impact of ozone on the growth and yield of trees. Journal of Environmental Quality 17, 347–360.
Regener, V.H., 1957. The vertical flux of atmospheric ozone. Journal of Geophysical Research 62, 221–228.
Ridley, B.A., Shetter, J.D., Walega, J.G., Madronich, S., Elsworth, C.M., Grahek, F.E., Fehsenfeld, F.C., Norton, R.B., Parrish, D.D., Hübler, G., Buhr, M., Williams, E.J., Allwine, E.J., Westberg, H.H., 1990. The behavior of some organic nitrates at Boulder and Niwot Ridge, Colorado. Journal of Geophysical Research 95, 13949–13961.
Rinne, H.J.I., Delany, A.C., Greenberg, J.P., Guenther, A.B., 2000. A true eddy accumulation system for trace gas fluxes using disjunct eddy sampling method. Journal of Geophysical Research 105, 24791–24798.
Rondón, A., Johansson, C., Granat, L., 1993. Dry deposition of nitrogen dioxide and ozone to coniferous forests. Journal of Geophysical Research 98, 5159–5172.
Schäfer, K.V.R., Oren, R., Lai, C.-T., Katul, G., 2002. Hydrologic balance in an intact temperate forest ecosystem under ambient and elevated atmospheric CO_2 concentration. Global Change Biology 8, 895–911.
Thom, A.S., 1975. Momentum, mass and heat exchange in plant communities. In: Monteith, J.L. (Ed.), Vegetation and the Atmosphere. Academic, London, pp. 57–109.
Turnipseed, A.A., Huey, L.G., Nemitz, E., Stickel, R., Higgs, J., Tanner, D.J., Slusher, D.L., Sparks, J.P., Flocke, F., Guenther, A., 2006. Eddy covariance fluxes of peroxyacetyl nitrates (PANs) and NOy to a coniferous forest. Journal of Geophysical Research 111, D09304, doi:10.1029/2005JD006631.
Turnipseed, A.A., Anderson, D.E., Blanken, P.D., Baugh, W., Monson, R.K., 2003. Airflows and turbulent flux measurements in mountainous terrain. Part 1. Canopy and local effects. Agricultural and Forest Meteorology 119, 1–21.
Turnipseed, A.A., Blanken, P.D., Anderson, D.E., Monson, R.K., 2002. Surface energy balance above a high-elevation subalpine forest. Agricultural and Forest Meteorology 110, 177–201.
US EPA, 1996. Air Quality Criteria for Ozone and Related Photochemical Oxidants. EPA 600/P-93/004bF. Office of Research and Development, Washington, DC.
Vingarzan, R., 2004. A review of surface ozone background levels and trends. Atmospheric Environment 38, 3431–3442.
Wesely, M.L., 1989. Parameterization of surface resistances to gaseous dry deposition in regional-scale numerical models. Atmospheric Environment 23, 1293–1304.
Wesely, M.L., Hicks, B.B., 2000. A review of the current status of knowledge on dry deposition. Atmospheric Environment 34, 2261–2282.
Wesely, M.L., Eastman, J.A., Cook, D.R., Hicks, B.B., 1978. Day-time variations of ozone eddy fluxes to maize. Boundary-Layer Meteorology 15, 361–373.
Wilczak, J.M., Oncley, S.P., Stage, S.A., 2001. Sonic anemometer tilt correction algorithms. Boundary-Layer Meteorology 99, 127–150.
Yi, C., Monson, R.K., Zhai, Z., Anderson, D.E., Lamb, B., Allwine, G., Turnipseed, A.A., Burns, S.P., 2005. Modeling and measuring the nocturnal drainage flow in a high-elevation, subalpine forest with complex terrain. Journal of Geophysical Research 110, D22303, doi:10.1029/2005JD006282.
Zeller, K.F., Nikolov, N.T., 2000. Quantifying simultaneous fluxes of ozone, carbon dioxide and water vapor above a subalpine forest ecosystem. Environmental Pollution 107, 1–20.
Zhang, L., Brook, J.R., Vet, R., 2002. On ozone dry deposition—with emphasis on non-stomatal uptake and wet canopies. Atmospheric Environment 36, 4787–4799.